*Science of Sintering,* **45** (2013) 233-243

doi: 10.2298/SOS1302233V

UDK 622.785;676.017.2

# Improvement of the Mechanical Properties of Spark Plasma Sintered HAP Bioceramics by Decreasing the Grain Size and by Adding Multi-walled Carbon Nanotubes

**Dj. Veljović[1*)], G. Vuković[1], I. Steins[2], E. Palcevskis[2], P. S. Uskoković[1], R. Petrović[1], Dj. Janaćković[1]**

[1]Faculty of Technology and Metallurgy, University of Belgrade, Karnegijeva 4, 11120 Belgrade, Serbia

[2]Institute of Inorganic Chemistry, Riga Technical University, Miera 34, Salaspils, LV-2169, Riga, Latvia

***Abstract:***

*Composites based on HAP and oxidized multi-walled carbon nanotubes (o-MWCNT) and monophase HAP materials were processed by spark plasma sintering. Starting from stoichiometric nano-sized HAP powder, monophase bioceramics were obtained with a density close to the theoretical one and with an average grain size of several hundred nanometers to micron dimensions. It was shown that decreasing the sintering temperature resulted in a decrease of the grain size, which affected an increase in the fracture toughness and hardness. The fracture toughness of an HAP/ o-MWCNT bioceramic processed at 900 °C for only 5 min was 30 % higher than that of monophase HAP materials obtained under the same conditions. The addition of MWCNT during SPS processing of HAP materials caused a decrease in the grain size to the nano-dimension, which was one of the reasons for the improved mechanical properties.*

***Keywords****: Hydroxyapatite, Carbon nanotubes, Grain size, Nanocomposite, Mechanical properties.*

## 1. Introduction

Dense, controlled porous and scaffold forms of hydroxyapatite (HAP) bioceramics, prepared by different sintering methods, are often used as reparation material in maxillofacial, dental and orthopedic surgery. Despite its optimal chemical composition, bioactivity and excellent biocompatibility with hard tissues, the brittle nature of HAP materials limit there use in load-bearing clinical applications [1-5]. During sintering at relatively high temperatures, calcium-deficient apatite becomes a mixture of HAP and $\alpha$- or $\beta$-tricalcium phosphate (TCP) and the presence of TCP phases in HAP-based bioceramic materials is detrimental for their mechanical properties. Monophasic HAP materials have appreciably higher values of fracture toughness and hardness than biphasic HAP/TCP ones, and in order to avoid deterioration of these mechanical properties, the absence of the TCP in HAP materials is essential [6-9].

Noticeable improvements of the mechanical properties of monophase HAP bioceramics were based on the control of the density, grain size, pore size and shapes, or on

*) **Corresponding author**: djveljovic@tmf.bg.ac.rs

the addition of different tougher and fibrous micro- and nano-sized particles into the HAP matrix [10-14]. The fracture toughness of dense hydroxyapatite bioceramics is often lower than 1 MPa $m^{1/2}$, which is significantly lower than the minimum reported value for natural bone (2 MPa $m^{1/2}$), and fracture toughness of synthesized HAP needs to be improved [3, 14]. An increase of fracture toughness with decreasing grain size is usually observed in the case of ceramics with intergranular fracture. By reduction of the grain size, the fraction of the grain boundary phase is increased and thereby a greater amount of energy is absorbed during crack propagation [8, 11, 15–17]. Some previous studies showed that the mechanical properties of monophase HAP materials were highly improved on reduction of the grain size from the micro to the nano level by decreasing the conventional sintering and hot pressing temperatures [8, 18]. In addition, it was shown that biocompatibility of the materials was improved by reduction of the grain size [19-22].

In order to decrease the sintering temperature, but still achieve materials of high density, pressure-assisted sintering is highly desirable, due to its enhancement of the densification kinetics and the curbing of grain growth. Spark plasma sintering (SPS) was found to show great potential in bioceramic processing, because this technique enables very high density to be attained while maintaining a very fine microstructure in very short processing times [23, 24]. Instead of an external heating source, the raw powder is heated from inside and outside using of a pulsed, direct current passing through the electrically conducting pressure die and through the sample. SPS is a rapid densification technique that promotes neck growth between the particles, thereby efficiently increasing their sinterability [10, 25].

On the other hand, the mechanical properties of HAP materials were improved by the addition of carbon nanotubes (CNTs), alumina ($Al_2O_3$), yttria-stabilized zirconia (YSZ), $Ni_3Al$ or Ti-alloys [13, 14, 26-28]. Carbon nanotubes have attracted great interest in most areas of nanoscience and nanotechnology due to their high chemical and thermal stability, mechanical strength, flexibility and electrical and thermal conductivity [29-31]. Incorporation of even small amounts of CNTs into a ceramic matrix is expected to produce composites with high stiffness and improved mechanical properties compared to the single-phase ceramic material. HAP/CNT composite materials have been prepared by conventional sintering, hot isostatic pressing and spark plasma sintering [32]. It was shown in all cases that the resulting composite materials had improved mechanical properties and biocompatibility. Li *et al*. [33] investigated the influence of the sintering atmosphere on mechanical properties of HAP and composite materials of HAP and 3 % of multi-walled CNT (MWCNTs), obtained by conventional sintering at 1100 ºC, for 3 h. They showed that the interface between MWCNTs and HAP in material obtained under vacuum was very strong and there were fewer pores in comparison to the material obtained in argon. By hot isostatic pressing, Kealley *et al*. [34] obtained a high density composite HAP/2 % CNT material that was biocompatible and had high mechanical strength and resilience [34]. Neutron diffraction patterns showed that the nanotubes have remained intact within the structure and that the CNTs had no effect on the structural parameters of the HAP phase, with the exception of a slight reduction in the unit cell parameter *a*. Determining the optimum sintering conditions of CNT modified HAP to obtain HAP/2 % CNT composite with improved mechanical properties using a spark plasma sintering system was the subject of the work of Xu *et al* [35]. To disperse the nanotubes homogeneously in the HAP, the CNT were mixed with spray-dried HAP powder in ethanol and mechanically stirred for even 5 days. The sintering temperatures were in the range 900–1200 °C with a dwell time of 3 min. The highest values of the Young's modulus and hardness were obtained for the material obtained by sintering at 1100 °C. At lower sintering temperatures porous materials were obtained, while there was significant grain growth at higher ones. A carbon nanotube- reinforced hydroxyapatite composite was also synthesized by Lahiri *et al*. [32], using spark plasma sintering at 1100 °C for 5 min. Quantitative microstructural analysis suggested that CNTs played a role in grain boundary pinning and

were responsible for the improved densification and retention of nanostructure throughout the thickness of the sintered pellet. The uniform distribution of 4 wt. % CNTs in the HAP matrix, good interfacial bonding and fine HAP grain size helped to improve the fracture toughness by 92 % and elastic modulus by 25 % as compared to the HAP matrix without CNTs.

It was shown in previous papers that the most important issues for preparing CNT/ceramic composites with high performances are homogenous mixing of the CNTs and ceramic powders, retention of the perfect structure of the CNTs during preparation of composites and strong interfacial bonding between the CNTs and the matrix to ensure load transfer [27, 32]. A common technique to improve the dispersion and realize the great capability of CNTs is chemical functionalization, which enables chemical covalent or non-covalent bonding between the CNTs and the matrix material [36, 37].

The aim of the present research was to obtain dense fine-grained monophase HAP and HAP/carbon nanotubes composite materials with improved mechanical properties by spark plasma sintering. The influence of decreasing the grain size by decreasing the sintering temperature and the addition of oxidized MWCNTs on the fracture toughness and hardness of the resulting materials were investigated.

## 2. Materials and methods

Nano-sized stoichiometric calcium hydroxyapatite powder (HAP) was synthesized by a chemical precipitation method described previously [11]. As reported in an earlier study, the Ca/P ratio of the HAP powder was 1.67, which showed that the starting hydroxyapatite powder was stoichiometric [8]. The XRD analysis showed the presence of calcium hydroxyapatite as the only crystalline phase [8]. The crystallite size was 35 nm [11]. TEM analysis showed agglomerates consisting of nano-sized rod-shaped particles 50–100 nm in size [11].

Multi-walled CNTs (MWCNT, Sigma-Aldrich) were oxidized according to a previous study [37]. Transmission electron microscopy analysis of the oxidized MWCNTs (o-MWCNT) was performed on a TECNAI-FEG F20 electron microscope at 200 kV.

To disperse homogeneously in the HAP powder, 1 or 3 wt. % of the o-MWCNT were sonicated for 3 h with HAP powder in ethanol and then mechanically stirred for 1 day. The dispersed mixture was then vacuum-filtered and dried at 110 °C for 8 h.

Spark plasma sintering was realized in a Dr Sinter SPS System-825C furnace. The pure HAP samples were sintered for 5 or 10 min at temperatures of 1200, 1000 or 900 ºC, while the HAP/o-MWCNT composite powders were sintered at 900 ºC for 5 min. Approximately 3 g of powder were sintered under vacuum using of graphite mold ($d$ = 20 mm) with an applied pressure of 40 MPa. During sintering, the voltage was 4 V with a current of 1500 A. The temperature of the sample during the sintering process was measured by optical pyrometers through a hole located in the graphite mold. After completion of the process, the samples were cooled for 1 h using the internal cooling system.

The XRD patterns of the sintered samples were recorded using a Bruker D8 Advance diffractometer. The patterns were collected at 25 ºC in the $2\theta$ range 20° to 50° with a scanning step of 0.02º. The densities of the sintered samples were measured by the Archimedes method. The morphology of the sintered samples was observed by a scanning electron microscope (SEM), Jeol JSM 5800, operated at 20 keV. The grain size of the sintered materials was measured by image analysis of the SEM micrographs, using the Image Pro Plus Program, version 4.0 for Windows. More than 100 grains from three sections were measured. The mechanical measurements were performed on polished sintered samples, with applied load of 1 kg for 10 s, using a Buehler Indentament 1100 series, Vickers Indentation Hardness Tester. The $K_{IC}$ values were calculated according the Evans–Charles Formula [38]: $K_{IC} = 0.0824\ P{\cdot}c^{-3/2}$, where $P$ is the indentation load and $c$ is the length of the induced radial crack.

## 3. Results and discussion

A TEM image of the o-MWCNT is shown in Fig. 1A, while a photograph of a dispersion of o-MWCNT in ethanol at a concentration of 1 mg $ml^{-1}$, taken 6 h after the solution had been sonicated for 1 h, is shown in Fig. 1B.

Compared with the raw MWCNTs [37], the sidewalls of the o-MWCNT were corrugated with carboxylated carbonaceous fragments on the outer graphite sheets, as shown in Fig. 1A by the arrow. The dispersibility of the o-MWCNTs (Fig. 1B) was remarkably better than that of the raw MWCNTs [37]. The oxidation introduced polar groups on the surface of the MWCNTs and therefore, created the electrostatic stability required for long-time stable dispersion in polar solvents [39-41]. The good dispersibility of the oxidized MWCNTs in solvents opened the path for their facile manipulation and processing in ceramic matrices. In addition, if CNTs are to be incorporated into composites for medical applications, evidence of their bioactivity and toxicity is essential. It was demonstrated previously [37] that the oxidized MWCNTs, at a concentration between 1 and 50 μg $ml^{-1}$, were not cytotoxic for the fibroblast L929 cell line.

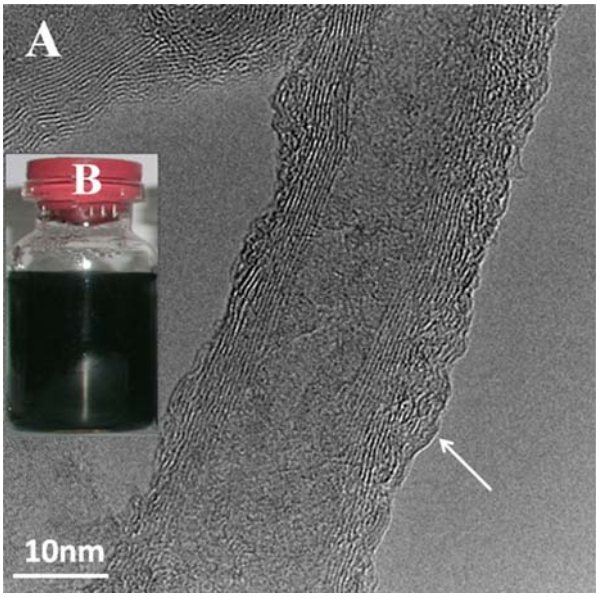


**Fig. 1.** A - Representative TEM image of the o-MWCNTs;
B - Dispersion of the o-MWCNTs in ethanol.

In order to obtain dense, fine-grained HAP materials, first, the pure HAP powder was SPS sintered at different temperatures and times: 1200 ºC for 5 min, 1000 ºC for 10 min and 900 ºC for 5 min. The XRD patterns of the obtained materials are shown in Fig. 2. All the XRD patterns are in agreement with the card JCPDS 9-432 and unequivocally shows that monophase HAP ceramics were obtained by SPS sintering, *i.e.,* the phase transformation of HAP to the TCP phase did not occur.

The density of the HAP-1200 was 3.03 ± 0.01 g/$cm^3$ (96 % TD). At the surface of this sample, micron size cracks were visible (it was not shown), because this temperature was too high for the sintering of nanosized HAP powder under SPS conditions. On decreasing the sintering temperature to 1000 ºC, the density of the HAP reached a value near the theoretical one (3.12±0.01 g/$cm^3$, *i.e.,* 99 % of the TD). The density of the sample obtained by sintering at 900 ºC was 2.85±0.02 g/$cm^3$ (≈ 91 % of the TD). According to these results, it could be said that a temperature of 1000 ºC was optimal for SPS sintering of the HAP powder.

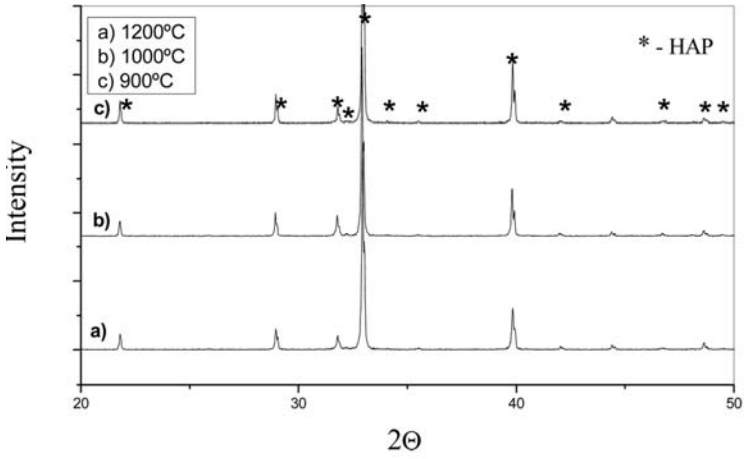


**Fig. 2.** XRD patterns of HAP samples SPS sintered at 1200 ºC for 5 min (HAP-1200), 1000 ºC for 10 min (HAP-1000) and 900 ºC for 5 min (HAP-900).

The microstructures of the fracture section of the obtained HAP materials are shown in Figs. 3(a-c). A non-uniform grain size distribution and grains of size between 10 and 20 μm are visible in microstructure of HAP-1200. The grain size distribution in the sample HAP-1000 is also non uniform (Fig. 3(b)), but the grain size was smaller, between 1-7 μm. On decreasing the sintering temperature to 900 ºC, the grain size of the HAP material definitely decreased; the grains were a few hundred nanometers in size (Fig. 3(c)).

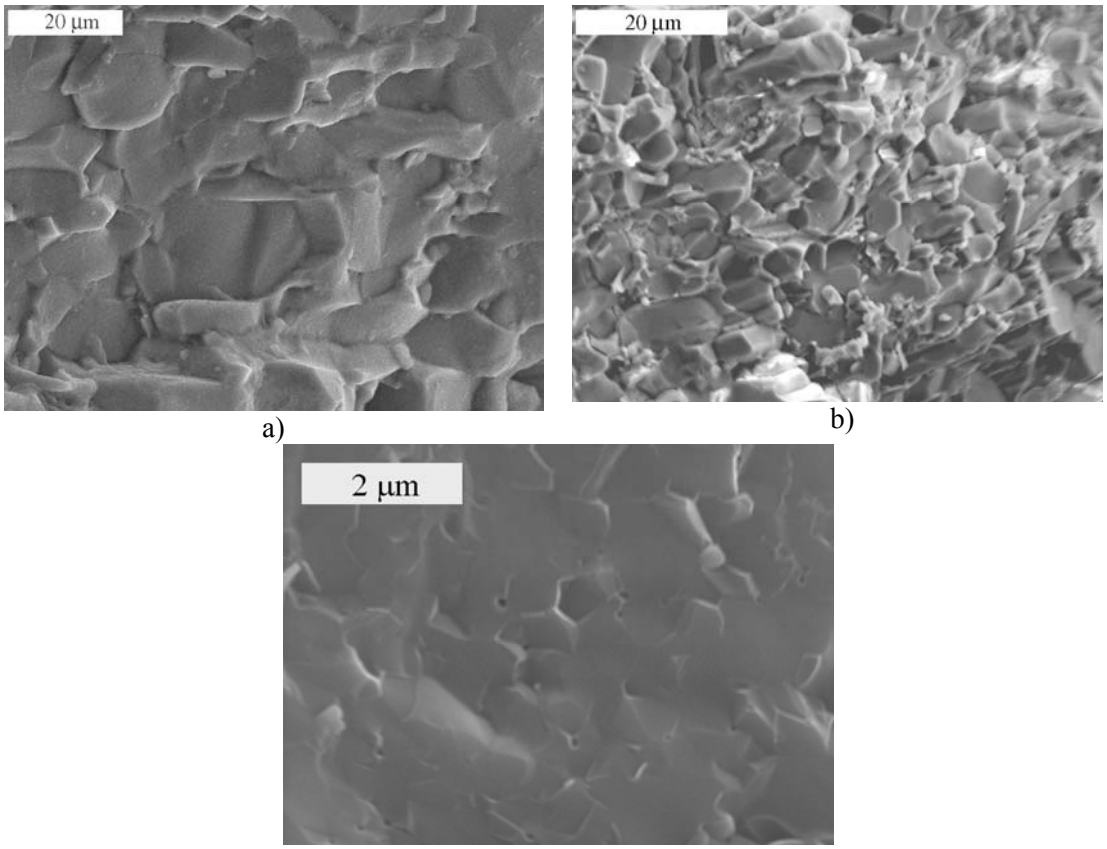


a) b)

c)

**Fig. 3.** SEM micrographs of (a) HAP-1200, (b) HAP-1000 and (c) HAP-900.

Mechanical properties of HAP-1200, HAP-1000 and HAP-900, together with mechanical properties of composite materials of HAP with 1 % o-MWCNT (HAP/1% o-MWCNT) and 3 % o-MWCNT (HAP/3% o-MWCNT), sintered at 900 ºC, are presented in Tab. I. The mechanical properties of the pure HAP materials were greatly improved by decreasing the sintering temperature. The material obtained by sintering at 1200 ºC had very poor mechanical properties, because there were micron size cracks in the material, as stated above. Despite the fact that the density of the material obtained by sintering at 900 ºC was much lower then that of the material obtained by sintering at 1000 ºC, the mechanical properties of this material were much better. According to this, it seems that the grain size was decisive for the mechanical properties of the pure HAP materials. The increase in fracture toughness was previously explained by the change of the fracture mechanism from transgranular to intergranular with decreasing grain size, whereby the cracks spread-out through the grain boundaries and the cracks become shorter due to the higher resistance of the larger number of grain boundaries [11]. The Hall-Petch Relation explains the increasing hardness with decreasing mean grain size of HAP bioceramics [6]. The present study showed that rapid SPS sintering at lower temperatures for very short holding times could produce fine-grained HAP ceramics with improved fracture toughness and hardness compared to HAP ceramics processed at higher temperatures.

**Tab. I** Processing conditions and mechanical properties of the SPS bioceramic materials.

| Phase composition | Sintering temperature, ºC | Time, min | Hardness, GPa | Fracture toughness, MPa $m^{1/2}$ |
|---|---|---|---|---|
| Pure HAP | 1000 | 10 | 2.30±0.18 | 0.80±0.05 |
| | 900 | 5 | 4.75±0.10 | 1.00±0.05 |
| HAP/1 % CNT | 900 | 5 | 4.10±0.15 | 1.15±0.08 |
| HAP/3 % CNT | 900 | 5 | 4.70±0.15 | 1.30±0.07 |

As the best mechanical properties of the pure HAP were achieved by SPS sintering at 900 ºC, this material was chosen for the investigation of the influence of o-MWCNTs on the microstructure and mechanical properties of HAP. The fracture toughness of composite materials was increased by 1 % of o-MWCNT addition (Table 1), while the hardness was lower than that of HAP-900. However, in the case of HAP/3% o-MWCNT, the hardness was approximately the same as that of HAP-900, while the fracture toughness was 30 % higher than that of HAP-900. Obviously, the mechanical properties of the HAP material were improved by the addition of 3 % of o-MWCNT. The indentation fracture toughness of the HAP/3 % o-MWCNT composite sample SPS sintered at 900 ºC was appreciably higher than those reported in many studies for micro- and nano-structured dense mono and biphasic bioceramics processed by spark plasma sintering, hot pressing and conventional sintering [3, 10, 18, 42].

The XRD pattern of the HAP/3% o-MWCNT presented in Fig. 4., confirmed that the addition of 3 % o-MWCNT did not initiate phase transformation of HAP into TCP, *i.e.*, only HAP was present as the bioactive phase in the composite material SPS sintered at 900 ºC.

In the SEM micrograph of the HAP/3% o-MWCNT (Fig. 5.), it can be seen that a uniform distribution of o-MWCNT in a relatively dense HAP matrix was achieved by spark plasma sintering at 900 ºC. The carbon nanotubes and the HAP grains are presented at the fracture surface of the HAP/3 % o-MWCNT. It was supposed that the formation of chemical bonds between o-MWCNT and HAP, *e.g.* hydrogen bonding, and/or the carboxyl–calcium–carboxyl ([–$COO^-$]–$Ca^{2+}$–[–$COO^-$]) complex [37], allowed for uniform dispersion of the o-MWCNT in the HAP matrix.

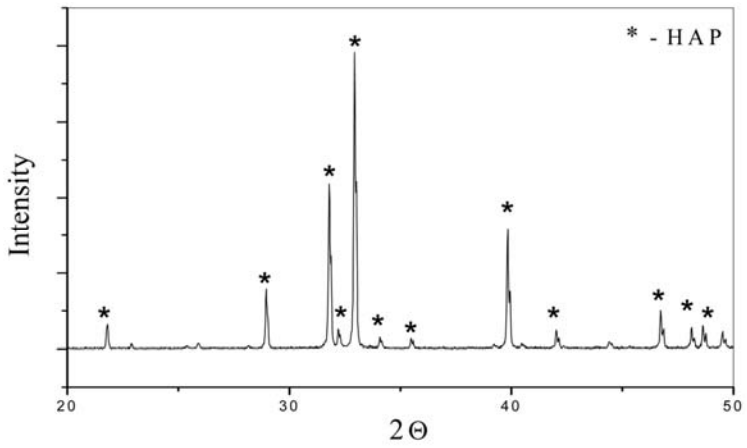


**Fig. 4.** XRD patterns of the HAP/o-MWCNT sample SPS sintered at 900 ºC for 5 min.

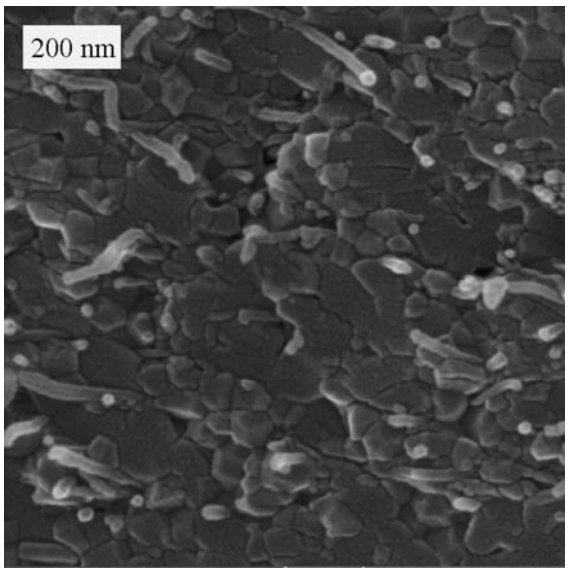


**Fig. 5.** The fracture surface of HAP/3 % o-MWCNT spark plasma sintered compact.

The fracture surface of HAP/3% o-MWCNT (Fig. 5.) shows that the pull-out carbon nanotubes were intergranularly incorporated into the HAP matrix. In comparison to the sample HAP-900 (Fig. 3(c)), the grains of the HAP/3% o-MWCNT are significantly smaller, with average grain size of 89±11 nm (Fig. 5.). This decrease of the grain size to the nano level can be linked to the presence of carbon nanotubes on the grain boundaries during grain growth.

The increasing of fracture toughness of the HAP material on addition of carbon nanotubes could be explained by the influence of the decrease in grain size and the presence of the relatively tough o-MWCNTs on the intergranular path of a potential crack. The addition of o-MWCNT, on the one hand, definitely affects a decrease in the HAP grain size and, on the other, as tough nano-particles, probably directly improved the fracture toughness of the composite. The MWNTs and grains formed a nano-grained matrix as can be seen at the fractured surface shown in Fig. 5., which was confirmation for the successful transfer of the load from the HAP matrix to the nanotubes, giving an explanation for the improvement of the fracture toughness. This combination of relatively high values of fracture toughness and hardness showed that controlling of the grain size and the simultaneous addition of o-

MWCNT into the spark plasma sintered HAP matrix, at relatively low temperatures, has great potential for improvement of the mechanical properties of bioceramic.

## 4. Conclusions

Starting from nano-sized HAP powder, monophase HAP bioceramic materials with a density close to the theoretical value and an average grain size of several hundred nanometers to micron dimensions were obtained by spark plasma sintering. It was shown that the reduction of the grain size of SPS HAP samples to the nano level instigated an increase in fracture toughness and hardness. By the addition of 3 % o-MWCNT, uniform nanocomposite bioceramics with improved fracture toughness were obtained by SPS at 900 ºC for 5 min. The fracture toughness of HAP/o-MWCNT composite biomaterial obtained at 900 ºC was 30 % higher in comparison to single-phase HAP material obtained under the same conditions, while the hardness of the material was similarly high. This study showed that the addition of carbon nanotubes during SPS processing of HAP materials caused a decrease in the grain size to nano-dimension, which is one of the reasons for the improvements of the mechanical properties of the resulting material.

## Acknowledgements

The authors wish to acknowledge the financial support for this research from Ministry of Education and Science of the Republic of Serbia through the project III45019 and FP7-REGPOT-2009-1 NANOTECH FTM, Grant Agreement Number: 245916, for financial support for the training of young researchers in the field of spark plasma sintering.

## 5. References

1. L. L. Hench, Bioceramics: from concept to clinic, J. Am. Ceram. Soc., 74 (1991) 1487.
2. R. Z. Legeros, J. P. Legeros, Dense hydroxyapatite, in An introduction to bioceramics, eds. L. L. Hench, and J. Wilson, World Scientific, Singapore, 1993, p. 139.
3. S. Raynaud, E. Champion, J. P. Lafon, D. Bernache-Assollant, Calcium phosphate apatites with variable Ca/P atomic ratio III. Mechanical properties and degradation in solution of hot pressed ceramics, Biomaterials, 23 (2002) 1081.
4. D. Lahiri, S. Ghosh, A. Agarwal, Carbon nanotube reinforced hydroxyapatite composite for orthopedic application: A review, Mater. Sci. Eng. C, 32 (2012) 1727.
5. A. Amera, A. M. A. Abudalazez, A. Rashid Ismail, N. Hayati Abd Razak, S. Malik Masudi, S. Rizal Kasim, Z. Arifin Ahmad, Synthesis and Characterization of Porous Biphasic Calcium Phosphate Scaffold From Different Porogens For Possible Bone Tissue Engineering Applications, Sci. Sinter., 43 (2011) 183.
6. S. Raynaud, E. Champion, D. Bernache-Assollant, Calcium phosphate apatites with variable Ca/P atomic ratio II. Calcination and sintering, Biomaterials, 23 (2002) 1073.
7. C. Y. Tang, P. S. Uskokovic, C. P. Tsui, Dj. Veljovic, R. Petrovic, Dj. Janackovic, Influence of microstructure and phase composition on the nanoindentation characterization of bioceramic materials based on hydroxyapatite, Ceram. Int., 35 (2009) 2171.
8. Dj. Veljovic, I. Zalite, E. Palcevskis, I. Smiciklas, R. Petrovic, Dj. Janackovic,

Microwave sintering of fine grained HAP and HAP/TCP bioceramics, Ceram. Int., 36 (2010) 595.
9. H. Zhao, F. Wang, X. Chen, Z. Wei, D. Yu, Z. Jiang, The formation mechanism of the $\beta$-TCP phase in synthetic fluorohydroxyapatite with different fluorine contents, Biomed. Mater., 5 (2010) 045011.
10. Y. W. Gu, N. H. Loh, K. A. Khor, S. B. Tor, P. Cheang, Spark plasma sintering of hydroxyapatite powders, Biomaterials, 23 (2002) 37.
11. Dj. Veljovic, B. Jokic, R. Petrovic, E. Palcevskis, A. Dindune, I. N. Mihailescu, Dj. Janackovic, Processing of dense nanostructured HAP ceramics by sintering and hot pressing, Ceram. Int., 35 (2009) 1407.
12. Dj. Veljovic, E. Palcevskis, A. Dindune, S. Putic, I. Balac, R. Petrovic, Dj. Janackovic, Microwave sintering improves the mechanical properties of biphasic calcium phosphates from hydroxyapatite microspheres produced from hydrothermal processing, J. Mater. Sci., 45 (2010) 3175.
13. R. Kumar, K. H. Prakash, P. Cheang, K. A. Khor, Microstructure and mechanical properties of spark plasma sintered zirconia-hydroxyapatite nano-composite powders, Acta. Mater., 53 (2005) 2327.
14. A. A. White, S. M. Best, I. A. Kinloch, Hydroxyapatite-carbon nanotube composites for biomedical applications: A review, Int. J. Appl. Ceram. Technol., 4 (2007) 1.
15. J. R. Groza, Nanosintering, Nanostruct. Mater., 12 (1999) 987.
16. Y. M. Chiang, D. P. Birnie, W. D. Kingery, Physical ceramics., John Wiley and Sons, New York, 1997, p. 477-485.
17. P. Van Landuyt, F. Li, J. P. Keustermans, J. M. Streydio, F.Delannay, E. Muting, The influence of high sintering temperatures on the mechanical properties of hydroxyapatite, J. Mater.Sci.: Mater.Med., 6 (1995) 8.
18. J. Wang, L. L. Shaw, Nanocrystalline hydroxyapatite with simultaneous enhancements in hardness and toughness, Biomaterials, 30 (2009) 6565.
19. L. G. Gutwein, T. J. Webster, Osteoblast and chrondrocyte proliferation in the presence of alumina and titania nanoparticles, J. Nanoparticle Res., 4 (2002) 231.
20. S. A. Catledge, M. D. Fries, Y. K. Vohra, W. R. Lacefield, Nanostructured ceramics for biomedical implants, J. Nanosci. Nanotech., 2 (2008) 293.
21. S. Bose, S. Dasgupta, S. Tarafder, A. Bandyopadhyay, Microwave-processed nanocrystalline hydroxyapatite: Simultaneous enhancement of mechanical and biological properties, Acta Biomater., 6 (2010) 3782.
22. Dj. Veljovic, M. Colic, V. Kojic, G. Bogdanovic, Z. Kojic, A. Banjac, E. Palcevskis, R. Petrovic, Dj. Janackovic, The effect of grain size on the biocompatibility, cell-materials interface and mechanical properties of microwave sintered bioceramics, J. Biomed. Mater. Res. Part A, 100A (2012) 3059.
23. M. Demuynck, J. P. Erauw, O. Van der Biest, F. Delannay, F. Cambier, Densification of alumina by SPS and HP: A comparative study, J. Eur. Ceram. Soc., 32 (2012) 1957.
24. C. Lin, C. Xiao, Z. Shen, Nano Pores Evolution in Hydroxyapatite Microsphere during Spark Plasma Sintering, Sci. Sinter., 43 (2011) 39.
25. R. Kumar, P. Cheang, K. A. Khor, Spark plasma sintering and in vitro study of ultra-fine HA and $ZrO_2$–HA powders, J. Mater. Process. Technol., 140 (2003) 420.
26. Y. H. Meng, C. Y. Tang, C. P. Tsui, P. S. Uskokovic, Fabrication and Characterization of HA-$ZrO_2$-MWCNT Ceramic Composites, J. Compos. Mater., 44 (2010) 871.
27. H. Li, N. Zhao, Y. Liu, C. Liang, C. Shi, X. Du, J. Li, Fabrication and properties of carbon nanotubes reinforced Fe/hydroxyapatite composites by in situ chemical vapor deposition, Compos. Part A, 39 (2008) 1128.

28. T. Lei, L. Wang, C. Ouyang, N. F. Li, L. S. Zhou, In Situ Preparation and Enhanced Mechanical Properties of Carbon Nanotube/Hydroxyapatite Composites, Int. J. Appl. Ceram. Technol., 8 (2011) 532.
29. M. M. J. Treacy, T. W. Ebbesen, J. M. Gibson, Exceptionally high Young's modulus observed for individual carbon nanotubes, Nature, 381 (1996) 678.
30. E. W. Wong, P. E. Sheehan, C. M. Lieber, Nanobeam mechanics: Elasticity, strength, and toughness of nanorods and nanotubes, Science, 277 (1997) 1971.
31. F. Lupo, R. Kamalakaran, C. Scheu, N. Grobert, M. Ruhle, Microstructural investigations on zirconium oxide–carbon nanotube hybrid materials synthesized by hydrothermal crystallization, Carbon, 42 (2004) 1995.
32. D. Lahiri, V. Singh, A. K. Keshri, S. Seal, A. Agarwal, Carbon nanotube toughened hydroxyapatite by spark plasma sintering: Microstructural evolution and multiscale tribological properties, Carbon, 48 (2010) 3103.
33. A. Li, K. Sun, W. Dong, D. Zhao, Mechanical properties, microstructure and histocompatibility of MWCNTs/HAp biocomposites, Mater. Lett., 61 (2007) 1839.
34. C. Kealley, M. Elcombeb, A. van Riessenc, B. Ben-Nissan, Development of carbon nanotube-reinforced hydroxyapatite bioceramics, Physica B, 385–386 (2006) 496.
35. J. L. Xu, K. A. Khor, J. J. Sui, W. N. Chen, Preparation and characterization of a novel hydroxyapatite/carbon nanotubes composite and its interaction with osteoblast-like cells, Mater. Sci. Eng. C., 29 (2009) 44.
36. G. D. Vukovic, S. Z. Tomic, A. D. Marinkovic, V. Radmilovic, P. S. Uskokovic, M. Čolic, The response of peritoneal macrophages to dapsone covalently attached on the surface of carbon nanotubes, Carbon, 48 (2010) 3066.
37. G. Vukovic, A, Marinkovic, M. Obradovic, V. Radmilovic, M. Čolic, R. Aleksic, P. S. Uskokovic, Synthesis, characterization and cytotoxicity of surface amino-functionalized water-dispersible multi-walled carbon nanotubes, Appl. Surf. Sci., 255 (2009) 8067.
38. A. G. Evans, E. A. Charles, Fracture toughness determinations by indentation, J. Am. Ceram. Soc., 59 (1976) 371.
39. L. Wei, Y. Zhang, Covalent sidewall functionalization of single-walled carbon nanotubes: a photoreduction approach, Nanotechnology, 18 (2007) 495703.
40. V. Datsyuk, M. Kalyva, K. Papagelis, J. Parthenios, D. Tasis, A. Siokou, I. Kallitsis, C. Galiotis, Chemical oxidation of multi walled carbon nanotubes, Carbon, 46 (2008) 833.
41. A. G. Osorio, I. C. L. Silveira, V. L. Bueno, C. P. Bergmann, $H_2SO_4$/$HNO_3$/HCl-Functionalization and its effect on dispersion of carbon nanotubes in aqueous media, Appl. Surf. Sci., 255 (2008) 2485.
42. N. Thangamani, K. Chinnakali, F. D. Gnanam, The effect of powder processing on densification, microstructure and mechanical properties of hydroxyapatite, Ceram. Int., 28 (2002) 355.

***Садржај:*** *Композити на бази хидроксиапатита и оксидованих вишеслојних карбонских нанотуба и монофазни хидроксиапатитни материјали добијени су спарк плазма синтеровањем. Полазећи од стехиометријског наночестичног праха хидроксиапатита, добијени су монофазни хидроксиапатитни биокерамички материјали са густинама блиским теоријским вредностима и просечном величином зрна од неколико стотина нанометара до микронских димензија. Показано је да се са смањењем температуре синтеровања смањује просечна величина зрна, што утиче на повећање жилавости и тврдоће материјала. Жилавост композитног биокерамичког материјала добијеног на 900 °C за свега 5 минута била је 30 % већа од жилавости*

*монофазне хидроксиапатитне биокерамике добијене при идентичним параметрима процесирања. Додатак оксидованих карбонских нанотуба током процесирања спарк плазма синтеровањем, проузроковао је смањење величине зрна на ноно димензије, што је један од разлога за побољшање механичких својстава добијених материјала.*
***Кључне речи:*** *Хидроксиапатит, карбонске нанотубе, величина зрна, нанокомпозит, механичка својства.*